

Parametric resonance in a linear oscillator at square-wave modulation

Eugene I Butikov

St Petersburg State University, St Petersburg, Russia

E-mail: butikov@spb.runnet.ru

Received 23 July 2004, in final form 15 September 2004

Published 14 December 2004

Online at stacks.iop.org/EJP/26/157

Abstract

The phenomenon of parametric resonance in a linear torsion spring oscillator caused by a square-wave modulation of its moment of inertia is explained and investigated both analytically and with the help of a computer simulation. Characteristics of parametric resonance and regeneration are found and discussed in detail. Ranges of frequencies within which parametric excitation is possible are determined. Stationary oscillations at the boundaries of these ranges and at the threshold conditions are investigated.

1. Introduction: the investigated physical system

In a recent contribution to this journal [1] we suggested a simple physical system that perfectly suits the initial acquaintance with the basics of parametric resonance, namely, a torsion spring oscillator (figure 1) similar to the balance device of a mechanical watch. It consists of a rigid rod which can rotate about an axis that passes through its centre. Two identical weights are balanced on the rod. An elastic spiral spring is attached to the rod. The other end of the spring is fixed. When the rod is turned about its axis, the spring flexes. The restoring torque $-D\varphi$ of the spring is proportional to the angular displacement φ of the rotor from the equilibrium position. After a disturbance, the rotor executes natural harmonic torsional oscillations.

To provide modulation of a system parameter, we assume that the weights can be shifted simultaneously along the rod in opposite directions into other symmetrical positions so that the rotor as a whole remains balanced, but its moment of inertia J is changed. Periodic modulation of the moment of inertia by such mass redistribution can cause, under certain conditions, a growth of (initially small) natural rotary oscillations.

The right-hand side of figure 1 shows an electromagnetic analogue of the spring oscillator: a series *LCR*-circuit containing a capacitor, an inductor (a coil) and a resistor. Oscillating current can be excited by periodic changes of the inductance of the coil if we periodically

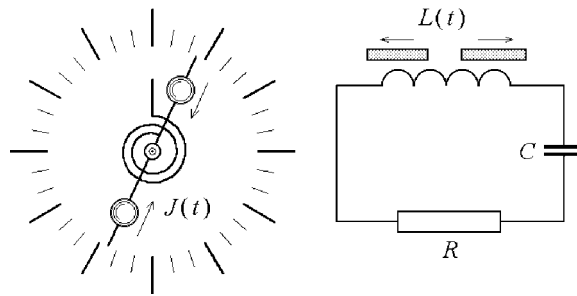


Figure 1. Schematic image of the torsion spring oscillator with a rotor whose moment of inertia is forced to vary periodically (left), and an analogous LCR -circuit with a coil whose inductance is modulated (right).

move an iron core in and out of the coil. Such periodic changes of the inductance are quite similar to the changes of the moment of inertia by mass redistribution in the mechanical system, which cause modulation of the natural frequency $\omega_0 = \sqrt{D/J}$ of the torsional oscillations of the rotor.

The suggested physical system is *linear* and hence has the advantage of simplicity compared, say, with a pendulum whose length is modulated (see, for example, [2–4]) or whose pivot is forced to move periodically up and down [5]. We have explained and quantitatively investigated in [1] the parametric excitation in this linear system caused by a *smooth* (sinusoidal) forced motion of the weights.

2. The square-wave modulation of the moment of inertia

This paper is concerned with a periodic *square-wave* modulation of the moment of inertia. The square-wave modulation provides an alternative and maybe a more straightforward way to understand and describe quantitatively the phenomenon of parametric resonance. A computer program [6] developed by the author simulates such a physical system and aids greatly in explaining the phenomenon.

In the case of the square-wave modulation, abrupt, almost instantaneous increments and decrements in the moment of inertia occur sequentially, separated by equal time intervals. We denote these intervals by $T/2$, so that T equals the period of the variation in the moment of inertia (the *period of modulation*). We can easily understand how the square-wave modulation can produce considerable oscillation of the rotor, if the period and phase of modulation are chosen properly.

For example, suppose that the weights are drawn closer to each other (and to the axis) at the instant at which the oscillating rotor passes through the equilibrium position, when its angular velocity is almost maximal. While the weights are being radially moved, the angular momentum of the system remains constant. Thus, the resulting reduction in the moment of inertia is accompanied by an increment in the angular velocity, and the rotor acquires additional energy. The greater the angular velocity, the greater the increment in energy. This additional energy is supplied by the source that moves the weights along the rod.

On the other hand, if the weights are instantly moved apart along the rotating rod, the angular velocity and the energy of the rotor diminish. The decrease in energy is transmitted back to the source. In order that increments in energy occur regularly and exceed the amounts of energy returned, i.e., in order that, as a whole, the modulation of the moment of inertia

regularly feeds the oscillator with energy, the period and phase of modulation must satisfy certain conditions.

For instance, let the weights be drawn closer to and moved apart from one another twice during one mean period of the natural oscillation. Furthermore, let the weights be drawn closer at the instant of maximal angular velocity, so that the rotor gains energy. After quarter period of the natural rotary oscillation the weights are moved apart, and this occurs almost at the instant of extreme deflection, when the angular velocity is nearly zero. Therefore, this particular motion causes no change in the angular velocity and kinetic energy of the rotor. Thus modulating the moment of inertia at a frequency twice the mean natural frequency generates the greatest growth of the amplitude, provided that the phase of the modulation is chosen in the way described above.

It is evident that the energy of the oscillator is increased not only when two full cycles of variation in the parameter occur during one natural period of oscillation, but also when two cycles occur during three, five or any odd number of natural periods. We shall see later that the delivery of energy, though less efficient, is also possible if two cycles of modulation occur during an even number of natural periods.

3. Conditions and peculiarities of parametric resonance

There are several important differences that distinguish parametric resonance from the ordinary resonance caused by an external force exerted directly on the system. Parametric resonance is possible when one of the following conditions for the frequency ω (or for the period T) of a parameter modulation is fulfilled:

$$\omega = 2\omega_0/n, \quad T = nT_0/2, \quad n = 1, 2, \dots \quad (1)$$

Parametric resonance is possible not only at the frequencies ω_n given in equation (1), but also in ranges of frequencies ω lying on either side of the values ω_n (in the *ranges of instability*). These intervals become wider as the depth of modulation is increased. An important difference between parametric excitation and forced oscillations is related to the dependence of the growth of energy on the energy already stored in the system. While for forced excitation the increment in energy during one period is proportional to the *amplitude* of oscillations, i.e., to the square root of the energy, at parametric resonance the increment in energy is proportional to the *energy* stored in the system.

Energy losses caused by friction are also proportional to the energy already stored. In the case of direct forced excitation energy losses restrict the growth of the amplitude because these losses grow with the energy faster than does the investment in energy arising from the work done by the external force. In the case of parametric resonance, both the investment in energy caused by the modulation of a parameter and the frictional losses are proportional to the energy stored, and so their ratio does not depend on the amplitude. Therefore, parametric resonance is possible only when a *threshold* is exceeded, that is, when the increment in energy during a period (caused by the parameter variation) is larger than the amount of energy dissipated during the same time. The critical (threshold) value of the modulation depth depends on friction. However, if the threshold is exceeded, the frictional losses of energy in a linear system cannot restrict the growth of the amplitude.

In a nonlinear system, the natural period depends on the amplitude of oscillations. If conditions for parametric resonance are fulfilled at small oscillations and the amplitude is growing, the conditions of resonance become violated at large amplitudes. In a real system the growth of the amplitude is restricted by nonlinear effects.

4. The threshold of parametric excitation

We can use arguments employing the conservation laws to evaluate the modulation depth which corresponds to the threshold of parametric excitation. Let the changes in the moment of inertia J of the rotor occur between maximal J_1 and minimal J_2 values equal to $J_0(1+m)$ and $J_0(1-m)$, respectively, where m is the dimensionless *depth of modulation*. During abrupt radial displacements of the weights along the rod, the angular momentum $L = J\omega$ of the rotor is conserved. Therefore, it is convenient to use the expression $E_{\text{kin}} = L^2/(2J)$, which gives the kinetic energy of the rotor in terms of L and J . For the increment ΔE in the rotor kinetic energy which occurs during an abrupt shift of the weights towards the axis, when the moment of inertia decreases from the value $J_1 = J_0(1+m)$ to the value $J_2 = J_0(1-m)$, we can write

$$\Delta E = \frac{L^2}{2J_0} \left(\frac{1}{1-m} - \frac{1}{1+m} \right) \approx 2m \frac{L^2}{2J_0} \approx 2m E_{\text{kin}}. \quad (2)$$

The approximate expressions in (2) are valid for small values of the modulation depth ($m \ll 1$). If the event occurs near the equilibrium position of the rotor, when the total energy E of the pendulum is approximately its kinetic energy E_{kin} , equation (2) shows that the fractional increment in the total energy $\Delta E/E$ approximately equals twice the value of the modulation depth m : $\Delta E/E \approx 2m$.

When the frequencies and phases have those values which are favourable for the most effective delivery of energy, the abrupt displacement of the weights toward the ends of the rod occurs at the instant when the rotor attains its greatest deflection (more precisely, when the rotor is very near it). At this instant the angular velocity of the rotor is almost zero, and so this radial displacement of the weights into their previous positions causes nearly no decrement in the energy.

For the principal resonance ($n = 1$) the investment in energy occurs twice during the natural period T_0 of oscillations. That is, the fractional increment in energy $\Delta E/E$ during one period approximately equals $4m$. A process in which the increment in energy ΔE during a period is proportional to the energy stored E ($\Delta E \approx 4mE$) is characterized on average by the exponential growth of the energy with time:

$$E(t) = E_0 \exp(\alpha t). \quad (3)$$

In this case, the index of growth α is proportional to the depth of modulation m of the moment of inertia: $\alpha = 4m/T_0$. When the modulation is exactly tuned to the principal resonance ($T = T_0/2$), the decrease of energy is caused almost only by friction. Dissipation of energy due to viscous friction during an integral number of natural cycles (for $t = nT_0$) is described by the following expression:

$$E(t) = E_0 \exp(-2\gamma t). \quad (4)$$

Comparing equations (3) and (4), we obtain the following estimate for the threshold (minimal) value m_{min} of the depth of modulation corresponding to the excitation of the principal parametric resonance:

$$m_{\text{min}} = \frac{1}{2} \gamma T_0 = \frac{\pi}{2Q}. \quad (5)$$

Here, we introduced the dimensionless quality factor $Q = \omega_0/(2\gamma)$ to characterize friction in the system.

The plot of the angular velocity and the phase trajectory of parametric oscillations occurring at the threshold conditions, equation (5), are shown in figure 2. This mode of

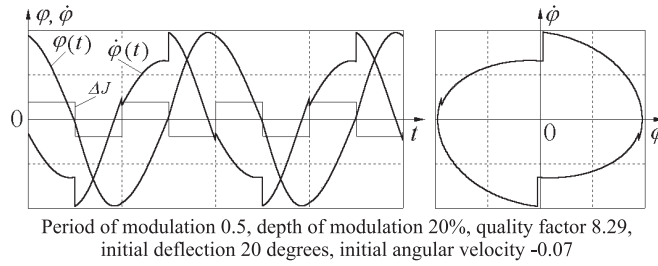


Figure 2. The time-dependent graphs and the phase trajectory of stationary oscillations at the threshold condition $m \approx \pi/2Q$ for $T = T_0/2$.

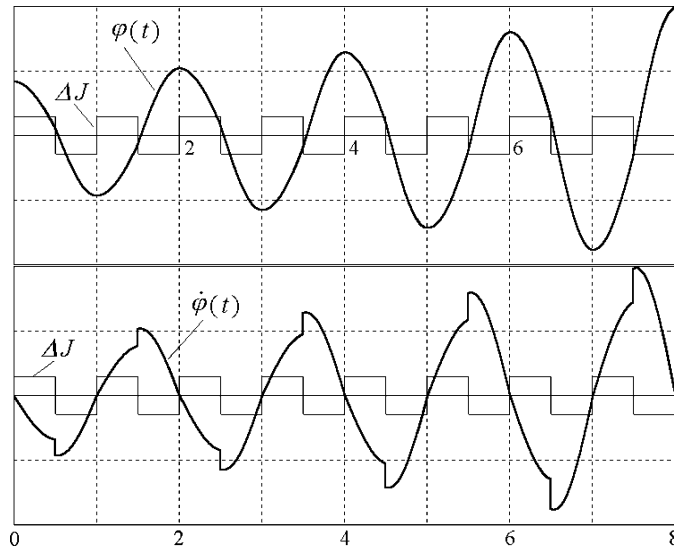


Figure 3. Exponential growth of the amplitude of oscillations at parametric resonance of the first order ($n = 1$).

steady oscillations (which have a constant amplitude in spite of the dissipation of energy) is called *parametric regeneration*.

For the third resonance ($T = 3T_0/2$) the threshold value of the depth of modulation is three times greater than its value for the principal resonance: $m_{\min} = 3\pi/(2Q)$. In this instance two cycles of the parametric variation occur during three full periods of natural oscillations. Radial displacements of the weights again happen at the most favourable moments, and so the same investment in energy occurs during an interval that is three times longer than the interval for the principal resonance.

When the depth of modulation exceeds the threshold value, the energy of oscillations increases exponentially with time. The growth of the energy again is described by equation (3). However, now the index of growth α is determined by the amount by which the energy delivered through parametric modulation exceeds the simultaneous losses of energy caused by friction: $\alpha = 4m/T_0 - 2\gamma$. The amplitude of parametrically excited oscillations also increases exponentially with time (figure 3): $a(t) = a_0 \exp(\beta t)$. The index β in the growth of amplitude is one-half the index of the growth in energy. For the principal resonance,

when the investment in energy occurs twice during one natural period of oscillation, we have $\beta = 2m/T_0 - \gamma = m\omega_0/\pi - \gamma$.

5. Differential equation for parametric oscillations

We next consider a more rigorous mathematical treatment of parametric resonance under square-wave modulation of the parameter. During the time intervals $(0, T/2)$ and $(T/2, T)$, the value of the moment of inertia is constant, and the motion of the rotor can be considered as a free oscillation described by a linear differential equation. However, the coefficients in this equation are different for the adjacent time intervals $(0, T/2)$ and $(T/2, T)$:

$$\ddot{\varphi} = -\frac{1}{1+m}(\omega_0^2\varphi + 2\gamma\dot{\varphi}) \quad \text{for } 0 < t < T/2, \quad (6)$$

$$\ddot{\varphi} = -\frac{1}{1-m}(\omega_0^2\varphi + 2\gamma\dot{\varphi}) \quad \text{for } T/2 < t < T. \quad (7)$$

Here, $\omega_0 = \sqrt{D/J_0}$ is the natural frequency of the oscillator and γ is the damping constant characterizing the strength of viscous friction. Both these quantities correspond to the mean value $J_0 = \frac{1}{2}(J_1 + J_2)$ of the moment of inertia. For small and moderate values of m the moment of inertia equals J_0 when the weights are near the half-way point between their extreme positions on the rod. For large m this is not the case because the moment of inertia depends on the square of the distance of the weights from the axis of rotation.

At each instant $t_n = nT/2$ ($n = 1, 2, \dots$) of an abrupt change in the moment of inertia we must make a transition from one of these linear equations (6) and (7) to the other. During each half-period $T/2$ the motion of the oscillator is a segment of some harmonic (or damped) natural oscillation. An analytical investigation of parametric excitation can be carried out by fitting to one or another known solution to the linear equations (6) and (7) for consecutive adjacent time intervals.

The initial conditions for each subsequent time interval are chosen according to the physical model in the following way. Each initial value of the angular displacement φ equals the value $\varphi(t)$ reached by the oscillator at the end of the preceding time interval. The initial value of the angular velocity $\dot{\varphi}$ is related to the angular velocity at the end of the preceding time interval by the law of conservation of the angular momentum:

$$(1+m)\dot{\varphi}_1 = (1-m)\dot{\varphi}_2. \quad (8)$$

In equation (8) $\dot{\varphi}_1$ is the angular velocity at the end of the preceding time interval, when the moment of inertia of the rotor has the value $J_1 = J_0(1+m)$, and $\dot{\varphi}_2$ is the initial value for the following time interval, during which the moment of inertia is equal to $J_2 = J_0(1-m)$. The change in the angular velocity at an abrupt variation of the inertia moment from the value J_2 to J_1 can be found in the same way.

That we may use the conservation of angular momentum, as expressed in equation (8), is allowed because, at sufficiently rapid displacement of the weights along the rotor, we can neglect the influence of the spring and consider the rotor as if it were freely rotating about its axis. This assumption is valid provided the duration of the displacement of the weights is a small portion of the natural period.

Considering conditions for which equations (6) and (7) yield solutions with increasing amplitudes, we can determine the ranges of frequency ω near the values $\omega_n = 2\omega_0/n$, within which the state of rest is unstable for a given modulation depth m . In these ranges of instability an arbitrarily small deflection from equilibrium is sufficient for the progressive growth of small initial oscillations.

6. The mean natural period at large depth of modulation

The threshold for the parametric excitation of the torsion pendulum is determined above for the resonant situations in which two cycles of the parametric modulation occur during one natural period or during three natural periods of oscillation. The estimate obtained, equation (5), is valid for small values of the modulation depth m .

For large values of the modulation depth m , the notion of a natural period needs a more precise definition. Let $T_0 = 2\pi/\omega_0 = 2\pi\sqrt{J_0/D}$ be the period of oscillation of the rotor when the weights are fixed in some middle positions, for which the moment of inertia equals J_0 . The period is somewhat longer when the weights are moved further apart: $T_1 = T_0\sqrt{1+m} \approx T_0(1+m/2)$. The period is shorter when the weights are moved closer to one another: $T_2 = T_0\sqrt{1-m} \approx T_0(1-m/2)$.

It is convenient to define the average period T_{av} not as the arithmetic mean $\frac{1}{2}(T_1 + T_2)$, but rather as the period that corresponds to the arithmetic mean frequency $\omega_{av} = \frac{1}{2}(\omega_1 + \omega_2)$, where $\omega_1 = 2\pi/T_1$ and $\omega_2 = 2\pi/T_2$. So we define T_{av} by the relation

$$T_{av} = \frac{2\pi}{\omega_{av}} = \frac{2T_1T_2}{T_1 + T_2}. \quad (9)$$

The period T of the parametric modulation which is exactly tuned to any of the parametric resonances is determined not only by the order n of the resonance, but also by the depth of modulation m . In order to satisfy the resonant conditions, the increment in the phase of natural oscillations during one cycle of modulation must be equal to $\pi, 2\pi, 3\pi, \dots, n\pi, \dots$. During the first half-cycle the phase increases by $\omega_1 T/2$, and during the second half-cycle by $\omega_2 T/2$. Consequently, instead of the approximate condition expressed by equation (1), we obtain

$$\frac{\omega_1 + \omega_2}{2} T = n\pi, \quad \text{or} \quad T = n \frac{\pi}{\omega_{av}} = n \frac{T_{av}}{2}. \quad (10)$$

Thus, for a parametric resonance of some definite order n , the condition for exact tuning can be expressed in terms of the two natural periods, T_1 and T_2 . This condition is $T = nT_{av}/2$, where T_{av} is defined by equation (9). For moderate values of m it is possible to use approximate expressions for the average frequency and period:

$$\omega_{av} = \frac{\omega_0}{2} \left(\frac{1}{\sqrt{1+m}} + \frac{1}{\sqrt{1-m}} \right) \approx \omega_0 \left(1 + \frac{3}{8}m^2 \right), \quad T_{av} \approx T_0 \left(1 - \frac{3}{8}m^2 \right).$$

The difference between T_{av} and T_0 reveals itself in terms proportional to the square of the depth of modulation m .

7. Frequency ranges for parametric resonances of odd orders

In order to determine the boundaries of the frequency ranges of parametric instability surrounding the resonant values $T = T_{av}/2, T = T_{av}, T = 3T_{av}/2, \dots$, we can consider *stationary oscillations* that occur when the period of modulation T corresponds to one of the boundaries. These stationary oscillations can be represented as an alternation of natural oscillations with the periods T_1 and T_2 . In the absence of friction, the graphs of such oscillations are formed by segments of non-damped sine curves with the corresponding periods.

7.1. Main interval of parametric instability

We examine first the vicinity of the principal resonance occurring at $T = T_{av}/2$. Suppose that the period T of the parametric variation is a little shorter than the resonant value $T = T_{av}/2$,

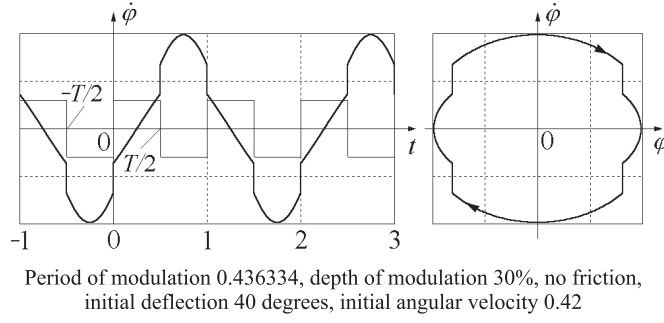


Figure 4. Stationary parametric oscillations at the lower boundary of the principal interval of instability (near $T = T_{av}/2$).

so that T corresponds to the left boundary of the interval of instability. In this case, a little less than a quarter of the mean natural period T_{av} elapses between consecutive abrupt increases and decreases of the moment of inertia. The graph of the angular velocity $\dot{\varphi}(t)$ for this periodic stationary process has the characteristic pattern shown in figure 4. The segments of the graphs of free oscillations (which occur during time intervals during which the moment of inertia is constant) are alternating parts of sine or cosine curves with the periods T_1 and T_2 . These segments are symmetrically truncated on both sides.

To find conditions at which such stationary oscillations take place, we can write the expressions for $\varphi(t)$ and $\dot{\varphi}(t)$ during the adjacent intervals in which the oscillator executes natural oscillations, and then fit these expressions to one another at the boundaries. Such fitting must provide a periodic stationary process.

We let the origin of time, $t = 0$, be the instant when the weights are shifted apart. The angular velocity is abruptly decreased in magnitude at this instant (see figure 4). Then during the interval $(0, T/2)$ the graph describes a natural oscillation with the frequency $\omega_1 = \omega_0/\sqrt{1+m}$. It is convenient to represent this motion as a superposition of sine and cosine waves whose constant amplitudes are A_1 and B_1 :

$$\begin{aligned}\varphi_1(t) &= (A_1 \sin \omega_1 t + B_1 \cos \omega_1 t), \\ \dot{\varphi}_1(t) &= (A_1 \omega_1 \cos \omega_1 t - B_1 \omega_1 \sin \omega_1 t).\end{aligned}\quad (11)$$

Similarly, during the interval $(-T/2, 0)$ the graph in figure 4 is a segment of natural oscillation with the frequency $\omega_2 = \omega_0/\sqrt{1-m}$:

$$\begin{aligned}\varphi_2(t) &= (A_2 \sin \omega_2 t + B_2 \cos \omega_2 t), \\ \dot{\varphi}_2(t) &= (A_2 \omega_2 \cos \omega_2 t - B_2 \omega_2 \sin \omega_2 t).\end{aligned}\quad (12)$$

To determine the values of constants A_1 , B_1 and A_2 , B_2 , we can use the conditions that must be satisfied when the segments of the graph are joined together, taking into account the periodicity of the stationary process. At $t = 0$ the angle of deflection is the same for both φ_1 and φ_2 : $\varphi_1(0) = \varphi_2(0)$. From this condition, we find that $B_1 = B_2$. We later denote these equal constants simply by B . The angular velocity at $t = 0$ undergoes a sudden change:

$$(1+m)\dot{\varphi}_1(0) = (1-m)\dot{\varphi}_2(0).$$

This condition gives us the following relation between A_2 and A_1 : $A_2 = kA_1 = kA$ (further on we denote A_1 simply as A), where we have introduced a dimensionless quantity k which depends on the depth of modulation m :

$$k = \sqrt{\frac{1+m}{1-m}}.$$

Equations for the constants A and B are determined by the conditions at the instants $-T/2$ and $T/2$. For stationary periodic oscillations, corresponding to the principal resonance (and to all resonances of odd numbers $n = 1, 3, \dots$ in equation (10)), these conditions are

$$\varphi_1(T/2) = -\varphi_2(-T/2), \quad (1+m)\dot{\varphi}_1(T/2) = -(1-m)\dot{\varphi}_2(-T/2). \quad (13)$$

Substituting φ and $\dot{\varphi}$ from equation (12) into equation (13), we obtain the system of homogeneous equations for the unknown quantities A and B :

$$\begin{aligned} (S_1 - kS_2)A + (C_1 + C_2)B &= 0, \\ k(C_1 + C_2)A - (kS_1 - S_2)B &= 0. \end{aligned} \quad (14)$$

In equation (14), the following notation is used:

$$\begin{aligned} C_1 &= \cos(\omega_1 T/2), & C_2 &= \cos(\omega_2 T/2), \\ S_1 &= \sin(\omega_1 T/2), & S_2 &= \sin(\omega_2 T/2). \end{aligned} \quad (15)$$

The homogeneous system of equations (14) for A and B has a non-trivial (non-zero) solution only if its determinant is zero:

$$2kC_1C_2 - (1+k^2)S_1S_2 + 2k = 0. \quad (16)$$

This condition for the existence of a non-zero solution to equation (14) gives us an equation for the unknown variable T , which enters equation (16) as the arguments of sine and cosine functions in S_1 , S_2 and C_1 , C_2 . This equation determines the desired boundaries of the interval of instability. These boundaries T_- and T_+ are given by the roots of equation (16). To find approximate solutions T to this transcendental equation, we transform it into a more convenient form. We first represent in equation (16) the products C_1C_2 and S_1S_2 as follows:

$$C_1C_2 = \frac{1}{2} \left(\cos \frac{\Delta\omega T}{2} + \cos \omega_{av} T \right), \quad S_1S_2 = \frac{1}{2} \left(\cos \frac{\Delta\omega T}{2} - \cos \omega_{av} T \right),$$

where $\Delta\omega = \omega_2 - \omega_1$. Then, using the identity $\cos \alpha = 2\cos^2(\alpha/2) - 1$, we reduce equation (16) to the following form:

$$(1+k) \cos \frac{\omega_{av} T}{2} = \pm |1-k| \cos \frac{\Delta\omega T}{4}. \quad (17)$$

For the boundaries of the instability interval which contains the principal resonance, we search for a solution T of equation (17) in the vicinity of $T = T_0/2$. For a given value of the depth of modulation m , equation (17) in the neighbourhood of $T_0/2 \approx T_{av}/2$ has two solutions which correspond to the boundaries T_- and T_+ of the instability interval. The graph of the angular velocity and the phase diagram for the right boundary of the main interval ($n = 1$) are shown in figure 5.

To find the boundaries T_- and T_+ of the instability interval, we replace T in the argument of the cosine on the left-hand side of equation (17) by $T_{av}/2 + \Delta T$, where $\Delta T \ll T_0$. Since $\omega_{av} T_{av} = 2\pi$, we can write the cosine as $-\sin(\omega_{av} \Delta T/2)$. Then equation (17) becomes

$$\sin \frac{\omega_{av} \Delta T}{2} = \mp \frac{|1-k|}{1+k} \cos \frac{\Delta\omega (T_{av}/2 + \Delta T)}{4}. \quad (18)$$

This equation for ΔT can be solved numerically by iteration. We start with $\Delta T = 0$ as an approximation of the zeroth order, substituting it into the right-hand side of equation (18), taken, say, with the upper sign. Then the left-hand side of equation (18) gives us the value of ΔT to the first order. We substitute this first-order value into the right-hand side of equation (18), and on the left-hand side we obtain ΔT to the second order. This procedure is iterated until a self-consistent value of ΔT for the left boundary is obtained.

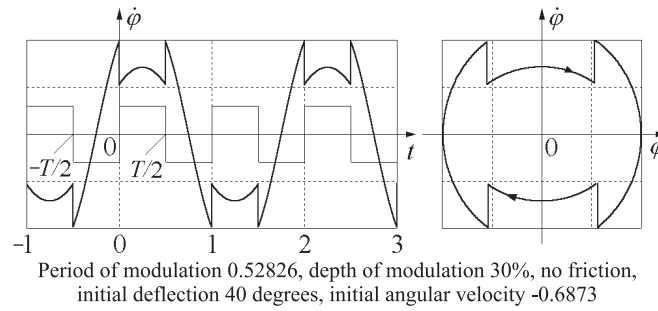


Figure 5. Stationary parametric oscillations at the upper boundary of the principal interval of instability (near $T = T_{av}/2$).

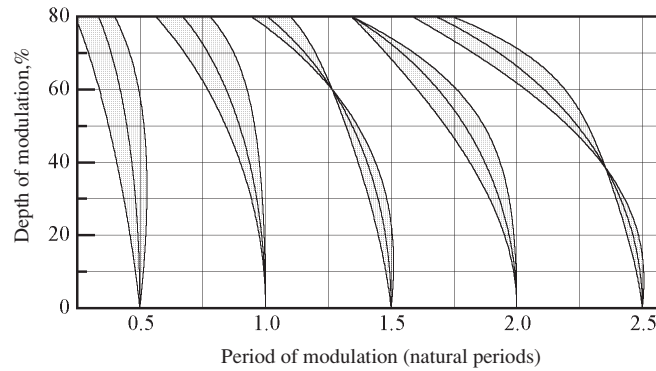


Figure 6. Intervals of parametric instability at square-wave modulation of the inertia moment in the absence of friction.

To determine ΔT for the right boundary (see figure 5), we use the same procedure, taking the lower sign on the right-hand side of equation (18).

After the substitution of one of the roots T_- or T_+ of equation (18) into (14) both equations for A and B become equivalent and allow us to find only the ratio A/B . This limitation means that the amplitude of stationary oscillations at the boundary of the instability interval can be arbitrarily large. This amplitude depends on the initial conditions. Nevertheless, these oscillations have a definite shape which is determined by the ratio of the amplitudes A and B of the sine and cosine functions whose segments form the pattern of the stationary parametric oscillation (see figures 4 and 5).

The intervals of instability for the first five parametric resonances are shown in figure 6 for various values of the modulation depth m . The diagram is obtained by the above-discussed numerical solution by iterations.

To obtain an approximate analytical solution to equation (18) that is valid for small values of the modulation depth m , we can simplify the expression on the right-hand side by assuming that $k \approx 1 + m$, $|1 - k| \approx m$. We may also assume the value of the cosine to be 1. On the left-hand side of equation (18), the sine can be replaced by its small argument, where $\omega_{av} = 2\pi/T_{av}$. Thus, we obtain the following approximate expression that is valid up to terms to the second order in m :

$$T_{\mp} = \frac{1}{2} \left(1 \mp \frac{m}{\pi} \right) T_{av} = \frac{1}{2} \left(1 \mp \frac{m}{\pi} - \frac{3m^2}{8} \right) T_0. \quad (19)$$

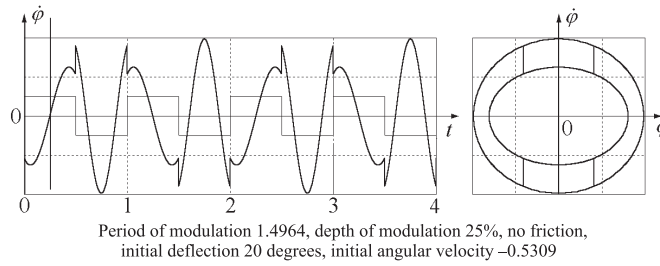


Figure 7. The graph of the angular velocity and the phase trajectory of stationary parametric oscillations at the left boundary of the interval of instability near $T = 3T_{av}/2$.

7.2. Third-order interval of parametric instability

In a similar way we can determine the boundaries of the instability interval in the vicinity of a resonance of the higher order $n = 3$. At this resonance two cycles of the parametric variation occur during three natural periods of oscillation ($T = 3T_{av}/2$). Considering stationary oscillations at the boundaries of the third interval (figure 7), we get the same equations (14) for A and B , as well as equation (17) for the values of the period of modulation. However, now we should search for a solution to equations (14) in the vicinity of $T = 3T_{av}/2$. The boundaries of this interval, obtained by a numerical solution, are also shown in figure 6.

For small values of the depth of modulation m , we can find approximate analytic expressions for the lower and the upper boundaries of the interval that are valid up to quadratic terms in m :

$$T_{\mp} = \left(\frac{3}{2} \mp \frac{m}{2\pi} \right) T_{av} = \left(\frac{3}{2} \mp \frac{m}{2\pi} - \frac{9m^2}{16} \right) T_0. \quad (20)$$

In this approximation, the third interval has the same width $(m/\pi)T_0$ as does the interval of instability in the vicinity of the principal resonance. However, this interval is distinguished by greater asymmetry: its central point is displaced to the left of the value $T = \frac{3}{2}T_0$ by $\frac{9}{16}m^2T_0$.

8. Frequency ranges for parametric resonances of even orders

For small and moderate square-wave modulation of the moment of inertia, parametric resonance of the order $n = 2$ (one cycle of the parametric variation during one natural period of oscillation) is relatively weak compared to the resonances $n = 1$ and $n = 3$ considered above. In the case in which $n = 2$ the abrupt changes of the moment of inertia induce both an increase and a decrease of the energy only once during each natural period. The growth of oscillations occurs only if the increase in energy at the instant when the weights are drawn closer is greater than the decrease in energy when the weights are drawn apart. This is possible only if the weights are shifted towards the axis when the angular velocity of the rotor is greater in magnitude than it is when they are shifted apart. For $T \approx T_{av}$, these conditions can be fulfilled only because there is a small difference between the natural periods T_1 and T_2 of the rotor, where T_1 is the period with the weights shifted apart and T_2 is the period with them shifted together. This difference is proportional to m .

The growth of oscillations at parametric resonance of the second order is shown in figure 8. In this case, the investment in energy during a period is proportional to the *square* of the depth of modulation m , while in the cases of resonances with $n = 1$ and $n = 3$ the investment in energy is proportional to the first power of m . Therefore, for the same value of

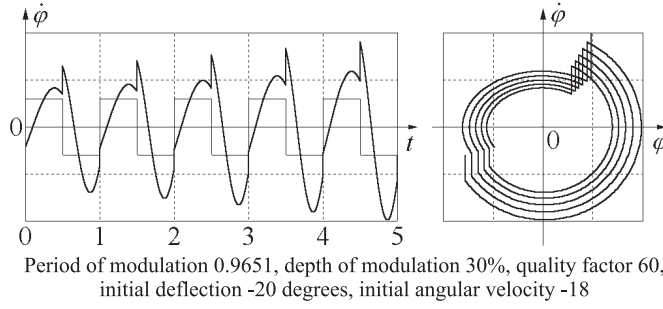


Figure 8. The graph of the angular velocity and the phase trajectory of oscillations corresponding to parametric resonance of the second order ($T = T_{av}$).

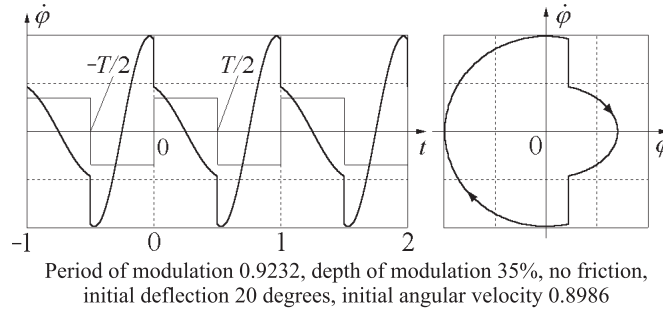


Figure 9. Stationary parametric oscillations at one of the boundaries of the interval of instability of the second order (near $T = T_{av} \approx T_0$).

the damping constant γ (the same quality factor Q), a considerably greater depth of modulation is required here to exceed the threshold of parametric excitation.

The interval of instability in the vicinity of resonance with $n = 2$ is considerably narrower compared to the corresponding intervals of the resonances with $n = 1$ and $n = 3$. Its width is also proportional only to the square of m (for small values of m).

To determine the boundaries of this interval of instability, we can consider, as is done above for other resonances, stationary oscillations for $T \approx T_0$ formed by alternating segments of free sinusoidal oscillations with the periods T_1 and T_2 . The graph of the angular velocity and the phase trajectory of such stationary periodic oscillations for one of the boundaries are shown in figure 9. During oscillations occurring at the boundary of the instability interval, the abrupt increment and decrement in the angular velocity exactly compensate each other.

To describe these stationary oscillations, we can use the same expressions for $\varphi(t)$ and $\dot{\varphi}(t)$ as we use in equations (11) and (12). The conditions for joining the graphs at $t = 0$ are also the same. However, differences begin with the equations for the constants A and B . They are determined by the conditions of periodicity at the instants $-T/2$ and $T/2$. For stationary periodic oscillations, corresponding to resonance with $n = 2$ (and for all resonances of even orders in equation (10)), these conditions are

$$\varphi_1(T/2) = \varphi_2(-T/2), \quad (1+m)\dot{\varphi}_1(T/2) = (1-m)\dot{\varphi}_2(-T/2), \quad (21)$$

and we obtain the system of equations for the amplitudes A and B :

$$\begin{aligned} (S_1 + kS_2)A + (C_1 - C_2)B &= 0, \\ k(C_1 - C_2)A - (kS_1 + S_2)B &= 0, \end{aligned} \quad (22)$$

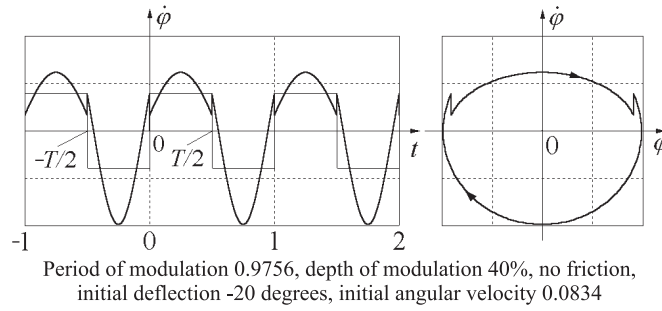


Figure 10. Stationary parametric oscillations at the other boundary of the interval of instability of the second order (near $T = T_{av} \approx T_0$).

where S_1 , C_1 and S_2 , C_2 are defined by the same equations (15). The homogeneous system of equations for A and B , equations (22), has a non-trivial solution if its determinant is zero:

$$2kC_1C_2 - (1 + k^2)S_1S_2 - 2k = 0. \quad (23)$$

In order to find the values $T_{\mp} = T_{av} + \Delta T$ for the instability interval with $n = 2$ from equation (23), we transform the products C_1C_2 and S_1S_2 in equation (23) by using the identity $\cos \alpha = 1 - 2 \sin^2(\alpha/2)$:

$$(1 + k) \sin \frac{\omega_{av} T}{2} = \pm |1 - k| \sin \frac{\Delta \omega T}{4}. \quad (24)$$

We next replace T in the argument of the sine on the left-hand side of equation (24) by $T_{av} + \Delta T$, where $\Delta T \ll T_0$. Since $\omega_{av} T_{av} = 2\pi$, we can write this sine as $-\sin(\omega_{av} \Delta T/2)$. Then equation (17) becomes

$$\sin \frac{\omega_{av} \Delta T}{2} = \mp \frac{|1 - k|}{1 + k} \sin \frac{\Delta \omega (T_{av} + \Delta T)}{4}. \quad (25)$$

This equation gives the left boundary T_- of the instability interval when we take the upper sign in its right-hand side, and the right boundary T_+ when we take the lower sign. Stationary oscillations, which correspond to the right boundary, are shown in figure 10.

Equation (25) for ΔT can also be solved numerically by iteration. Substituting T_- or T_+ obtained from (25) into one of the equations (14), we get the ratio of the amplitudes A and B that determines the pattern of stationary oscillations at the corresponding boundary of the instability interval. We note how narrow the intervals of even resonances ($n = 2, 4$) are for small values of m . With the growth of m the intervals expand and become comparable with the intervals of odd orders.

For small and moderate values of the depth of modulation, it is possible to find an approximate analytical solution to equation (25):

$$T_{\mp} = (1 \mp \frac{1}{4}m^2)T_{av} = T_0 + (\mp \frac{1}{4} - \frac{3}{8})m^2T_0, \quad (26)$$

i.e., $T_- = T_0 - \frac{5}{8}m^2T_0$, $T_+ = T_0 - \frac{1}{8}m^2T_0$. As mentioned above, the width $T_+ - T_- = \frac{1}{2}m^2T_0$ of this interval of instability is proportional to the square of the modulation depth.

9. Intersections of the boundaries at large modulation

Figure 6 shows that at some definite values of m both boundaries of intervals with $n > 2$ coincide (we may consider that they *intersect*). Thus, at these values of m the corresponding

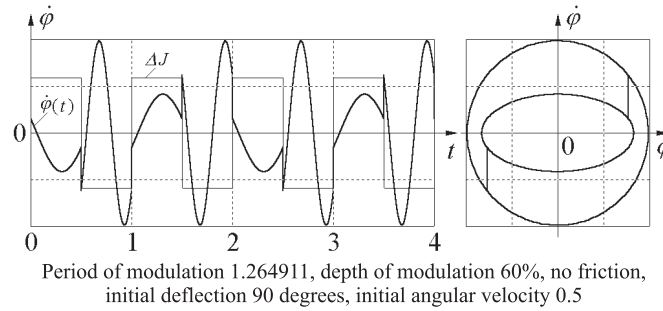


Figure 11. Time-dependent graph of the angular velocity and the phase trajectory for stationary oscillations at the intersection of both boundaries of the third interval.

intervals of parametric resonance disappear. These values of m correspond to the natural periods T_1 and T_2 of oscillation (associated with the weights far apart and close to each other), whose ratio is 2:1, 3:1 and 3:2.

For the first intersection (ratio 2:1) exactly one half of the natural oscillation with period T_1 is completed during the first half of the modulation cycle (see figure 11). On the phase diagram, the representing point traces a half of the smaller ellipse, and then abruptly jumps down to the larger ellipse. During the second half of the modulation cycle the oscillator executes exactly a whole natural oscillation with period $T_2 = T_1/2$, so that the representing point passes in the phase plane along the whole larger ellipse, and then jumps up to the smaller ellipse along the same vertical segment.

During the next modulation cycle the representing point generates first the other half of the smaller ellipse, and then again the whole larger ellipse. Therefore during any two adjacent cycles of modulation, the representing point passes once along the closed smaller ellipse and twice along the larger one, returning finally to the initial point of the phase plane. We see that such an oscillation is periodic for arbitrary initial conditions. This means that for the corresponding values of the modulation depth m and the period of modulation T the growth of amplitude is impossible even in the absence of friction (the instability interval vanishes).

Similar explanations can be suggested for other cases in figure 6 in which the boundaries intersect.

10. Intervals of parametric excitation in the presence of friction

When there is friction in the system, the intervals of the period of modulation become narrower, and for strong enough friction (below the threshold) the intervals disappear. Above the threshold, approximate values for the boundaries of the first interval are given by equation (19) provided we substitute for m the expression $\sqrt{m^2 - m_{\min}^2}$ with the threshold value $m_{\min} = \pi/(2Q)$ defined by equation (5). The proof can be found in appendix A. For the third interval, we can use equation (20), substituting $\sqrt{m^2 - m_{\min}^2}$ for m , with $m_{\min} = 3\pi/(2Q)$. When m is equal to the corresponding threshold value m_{\min} , the interval of parametric resonance disappears.

The boundaries of the second interval of parametric resonance in the presence of friction are approximately given by equation (26) provided we substitute for m^2 the expression $\sqrt{m^4 - m_{\min}^4}$ with the threshold value $m_{\min} = \sqrt{2/Q}$, which corresponds to the second parametric resonance (see appendix B).

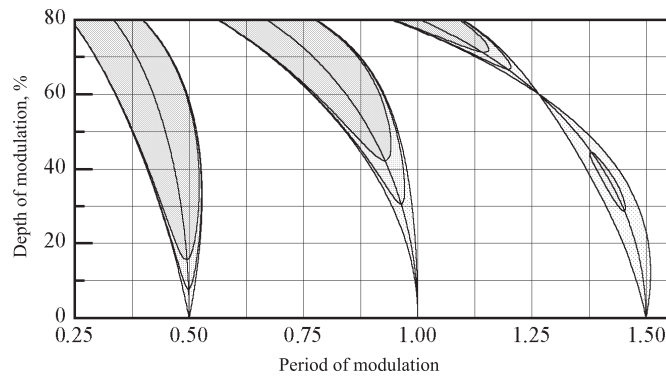


Figure 12. Intervals of parametric excitation at square-wave modulation of the moment of inertia without friction, for $Q = 20$ and for $Q = 10$.

The diagram in figure 12 shows the boundaries of the first three intervals of parametric resonance for $Q = 20$ and $Q = 10$ (and also in the absence of friction). Note the ‘island’ of parametric resonance for $n = 3$ and $Q = 20$. This resonance disappears when the depth of modulation exceeds 45% and reappears when m exceeds approximately 66%.

In the presence of friction, for any given value m of the depth of modulation, only several first intervals of parametric resonance (where m exceeds the threshold) can exist. We note that in case when the equilibrium of the system is unstable due to modulation of the parameter, parametric resonance can occur only if at least small oscillations are already excited. Indeed, when the initial values of φ and $\dot{\varphi}$ are exactly zero, they remain zero over the course of time. This behaviour is in contrast to that of resonance arising from forced oscillations, when the amplitude increases with time even if initially the system is at rest in the equilibrium position (if the initial conditions are zero).

11. Concluding remarks

We have shown above that a linear torsion oscillator whose moment of inertia is subjected to square-wave modulation by mass reconfiguration gives a very convenient example in which the phenomenon of parametric resonance can be clearly explained physically with all its peculiarities and even investigated quantitatively by rather modest mathematical means.

In a linear system, if the threshold of parametric excitation is exceeded, the amplitude of oscillations increases exponentially with time. In contrast to forced oscillations, linear viscous friction is unable to restrict the growth of the amplitude at parametric resonance. In real systems, the growth of the amplitude is restricted by nonlinear effects that cause the period to depend on the amplitude. During parametric excitation the growth of the amplitude causes variation of the natural period and thereby violates the conditions of resonance.

Appendix A. The principal interval of instability in the presence of friction

Stationary oscillations occurring at the left boundary of the instability interval in the vicinity of the principal parametric resonance in the presence of friction are shown in figure 13 (compare with figure 4). Twice during the full cycle the angular velocity abruptly increases, and twice it decreases. The increments are greater than the decrements, so that as a whole the energy received by the rotor exceeds the energy given away. This surplus compensates for the

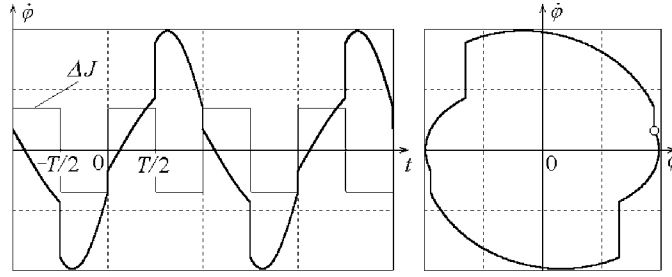


Figure 13. Stationary oscillations in the presence of friction at the left boundary of the principal instability interval.

dissipation of the energy which occurs for natural oscillation during the intervals between the abrupt displacements of the weights along the rod.

To find conditions at which such stationary oscillations take place, we can write the expressions for $\varphi(t)$ and $\dot{\varphi}(t)$ during the adjacent intervals when the oscillator executes damped natural oscillations, and then fit these expressions to one another at the boundaries. We choose as the time origin $t = 0$ the instant when the weights are shifted apart, and the angular velocity is decreased in magnitude. Then during the interval $(0, T/2)$ the graph describes a damped natural oscillation with the frequency $\omega_1 = \omega_0/\sqrt{1+m}$. Similarly to equation (11), it is convenient to represent this motion as a superposition of damped oscillations of sine and cosine types with some constants A_1 and B_1 :

$$\begin{aligned}\varphi_1(t) &= (A_1 \sin \omega_1 t + B_1 \cos \omega_1 t) e^{-\gamma t}, \\ \dot{\varphi}_1(t) &\approx (A_1 \omega_1 \cos \omega_1 t - B_1 \omega_1 \sin \omega_1 t) e^{-\gamma t}.\end{aligned}\quad (\text{A.1})$$

The latter expression for $\dot{\varphi}(t)$ is valid for relatively weak friction ($\gamma \ll \omega_0$). To obtain it, we differentiate $\varphi(t)$ with respect to the time, considering the exponential factor $e^{-\gamma t}$ to be approximately constant. Indeed, at weak damping the main contribution to the time derivative originates from the oscillating factors $\sin \omega_1 t$ and $\cos \omega_1 t$ in the expression for $\varphi(t)$. Similarly, during the interval $(-T/2, 0)$ the graph in figure 13 is a segment of damped natural oscillation with the frequency ω_2 :

$$\begin{aligned}\varphi_2(t) &= (A_2 \sin \omega_2 t + B_2 \cos \omega_2 t) e^{-\gamma t}, \\ \dot{\varphi}_2(t) &\approx (A_2 \omega_2 \cos \omega_2 t - B_2 \omega_2 \sin \omega_2 t) e^{-\gamma t}.\end{aligned}\quad (\text{A.2})$$

Further calculations are similar to those leading from equations (11) and (12) to (16), but instead of equation (16) we get the following equation:

$$2kC_1C_2 - (1+k^2)S_1S_2 + k(p+1/p) = 0, \quad (\text{A.3})$$

where the notation $p = e^{-\gamma T}$ is used. This condition of existence of a non-zero solution for constants A_1 and B_1 gives us an equation which determines the desirable boundaries of the interval of instability. These boundaries are given by the values of the unknown variable T (the roots of the equation), which enters equation (A.3) as the arguments of sine and cosine functions in S_1 , S_2 and C_1 , C_2 , and also as the argument of the exponent in $p = e^{-\gamma T}$. To find approximate solutions T to this transcendental equation, we transform it into a more convenient form in the same way as in section 5:

$$(1+k) \cos \frac{\omega_{av} T}{2} = \pm \sqrt{(1-k)^2 \cos^2 \frac{\Delta \omega T}{4} - k(p+1/p-2)}. \quad (\text{A.4})$$

To find the boundaries of the interval which contains the principal resonance, we should search for a solution T of equation (A.4) in the vicinity of $T = T_0/2 \approx T_{av}/2$. If for a given

value of the quality factor Q (Q enters $p = e^{-\gamma T}$) the depth of modulation m exceeds the threshold value, equation (A.4) has two solutions which correspond to the desirable boundaries T_- and T_+ of the instability interval. These solutions exist if the expression under the radical sign in equation (A.4) is positive. Its zero value corresponds to the threshold conditions:

$$\frac{(1-k)^2}{k} \cos^2 \frac{\Delta\omega T}{4} = p + 1/p - 2. \quad (\text{A.5})$$

To evaluate the threshold value of Q for small values of the modulation depth m , we may assume here $k \approx 1 + m$, and $\cos(\Delta\omega T/4) \approx 1$. On the right-hand side of equation (A.5), in $p = e^{-\gamma T}$, we can consider $\gamma T \approx \gamma T_0/2 = \pi/(2Q) \ll 1$, so that $p + 1/p - 2 \approx (\gamma T)^2 = (\pi/2Q)^2$. Thus, for the threshold of the principal parametric resonance we obtain

$$Q_{\min} \approx \frac{\pi}{2m} \left(1 + \frac{m}{2}\right) \approx \frac{\pi}{2m}, \quad m_{\min} \approx \frac{\pi}{2Q} \left(1 + \frac{\pi}{4Q}\right) \approx \frac{\pi}{2Q}. \quad (\text{A.6})$$

At the threshold the expression under the radical sign in equation (A.5) is zero. Both its roots (the boundaries of the instability interval) merge. This occurs when the cosine on the left-hand side of equation (A.5) is zero, that is, when its argument equals $\pi/2$:

$$\omega_{\text{av}} \frac{T}{2} = \frac{\pi}{2}, \quad \text{or} \quad T = \frac{\pi}{\omega_{\text{av}}} = \frac{1}{2} T_{\text{av}},$$

so that the threshold conditions (A.6) correspond to exact tuning to resonance, when $T = T_{\text{av}}/2$.

To find the boundaries T_- and T_+ of the instability interval, we represent T in the argument of the cosine function on the left-hand side of equation (A.4) as $T_{\text{av}}/2 + \Delta T$, where $\Delta T \ll T_0$. Since $\omega_{\text{av}} T_{\text{av}} = 2\pi$, this cosine can be written as $-\sin(\omega_{\text{av}} \Delta T/2)$. Then equation (A.4) becomes

$$\sin \frac{\omega_{\text{av}} \Delta T}{2} = \mp \frac{1}{1+k} \sqrt{(k-1)^2 \cos^2 \frac{\Delta\omega \left(\frac{1}{2} T_{\text{av}} + \Delta T\right)}{4} - k \frac{(p-1)^2}{p}}. \quad (\text{A.7})$$

For zero friction $p = 1$, and equation (A.7) coincides with (18). The diagram in figure 12 is obtained by numerically solving this equation for ΔT by iteration.

To obtain an approximate solution of equation (A.7), that is valid for small values of the modulation depth m up to terms to the second order of m , we can simplify the expression under the radical sign on the right-hand side of equation (A.4), assuming $k \approx 1 + m$, $(1-k)^2 \approx m^2$, and the value of the cosine function to be 1. The last term of the radicand can be represented as $(\pi/2Q)^2 \approx m_{\min}^2$. On the left-hand side the sine can be replaced with its small argument, where $\omega_{\text{av}} = 2\pi/T_{\text{av}}$. Thus, we obtain

$$\frac{\Delta T}{T_{\text{av}}} \approx \mp \frac{1}{2\pi} \sqrt{m^2 - m_{\min}^2}, \quad \text{or} \quad T_{\mp} = \frac{T_{\text{av}}}{2} \left(1 \mp \frac{1}{\pi} \sqrt{m^2 - m_{\min}^2}\right). \quad (\text{A.8})$$

For the case of zero friction $m_{\min} = 0$, and these approximate expressions for the boundaries of the instability interval reduce to equation (19). For the threshold conditions $m = m_{\min}$, and both boundaries of the interval merge, that is, the interval disappears.

Appendix B. The second interval of instability in the presence of friction

When friction is taken into account, we arrive at, instead of equation (24), the following equation for the boundaries of the second interval of parametric instability:

$$(1+k) \sin \frac{\omega_{\text{av}} T}{2} = \pm \sqrt{(1-k)^2 \sin^2(\Delta\omega T/4) - k(p + 1/p - 2)}. \quad (\text{B.1})$$

We should search for its solution T in the vicinity of $T = T_0 \approx T_{av}$. If for a given value of the quality factor Q (Q enters $p = e^{-\gamma T}$) the depth of modulation m exceeds the threshold value, equation (B.1) has two solutions which correspond to the boundaries T_- and T_+ of the instability interval. These solutions exist if the expression under the radical sign in equation (B.1) is positive. Its zero value corresponds to the threshold conditions:

$$\frac{(k-1)^2}{k} \sin^2(\Delta\omega T_{av}/4) = \frac{(p-1)^2}{p}. \quad (\text{B.2})$$

To estimate the threshold value of Q for small values of the modulation depth m , we may assume here $k \approx 1+m$, and $\sin(\Delta\omega T/4) \approx \Delta\omega T/4$. On the right-hand side of equation (B.2), in $p = e^{-\gamma T}$, we can consider $\gamma T \approx \gamma T_0 = \pi/Q \ll 1$, so that $p+1/p-2 = (p-1)^2/p \approx (\gamma T)^2 = (\pi/Q)^2$. Thus, for the threshold of the second parametric resonance we obtain

$$Q_{\min} \approx \frac{2}{m^2}, \quad m_{\min} \approx \sqrt{\frac{2}{Q}}. \quad (\text{B.3})$$

The threshold conditions correspond to exact tuning to resonance, when $T = T_{av}$.

To find the boundaries T_- and T_+ of the instability interval, we represent T in the argument of the sine function on the left-hand side of equation (B.1) as $T_{av} + \Delta T$, where $\Delta T \ll T_{av} \approx T_0$. Since $\omega_{av} T_{av} = 2\pi$, we can write this sine as $-\sin(\omega_{av} \Delta T/2)$. Then equation (B.1) becomes

$$\sin \frac{\omega_{av} \Delta T}{2} = \mp \frac{1}{1+k} \sqrt{(k-1)^2 \sin^2 \frac{\Delta\omega(T_{av} + \Delta T)}{4} - k \frac{(p-1)^2}{p}}. \quad (\text{B.4})$$

This form of the equation is convenient for numerical solution by iteration. For the zero friction $p = 1$, and equation (B.4) coincides with equation (25). To obtain an approximate solution of equation (B.4), valid for small values of the modulation depth m up to the terms of the second order of m , we can simplify the expression under the radical sign on the right-hand side of equation (B.4), assuming $k \approx 1+m$, $(1-k)^2 \approx m^2$, and $\sin \Delta\omega(T_{av} + \Delta T)/4 \approx \Delta\omega T_{av}$. The last term of the radicand can be represented as $(2/Q)^2 \approx m_{\min}^4$. On the left-hand side the sine can be replaced by its small argument, where $\omega_{av} = 2\pi/T_{av}$. Thus, for the boundaries of the second instability interval we obtain

$$\frac{\Delta T}{T_{av}} \approx \mp \frac{1}{4} \sqrt{m^4 - m_{\min}^4}, \quad \text{or} \quad T_{\mp} = \left(1 \mp \frac{1}{4} \sqrt{m^4 - m_{\min}^4} \right) T_{av}. \quad (\text{B.5})$$

References

- [1] Butikov E 2004 Parametric excitation of a linear oscillator *Eur. J. Phys.* **25** 535–54
- [2] Case W 1996 The pumping of a swing from the standing position *Am. J. Phys.* **64** 215–20
- [3] Pinsky M and Zevin A 1999 Oscillations of a pendulum with a periodically varying length and a model of swing *Int. J. Non-Linear Mech.* **34** 105–9
- [4] Stilling D and Szyskowski W 2002 Controlling angular oscillations through mass reconfiguration: a variable length pendulum case *Int. J. Non-Linear Mech.* **37** 89–99
- [5] Butikov E I 2001 On the dynamic stabilization of an inverted pendulum *Am. J. Phys.* **69** 755–68
- [6] Butikov E I 1996 Educational software package *Physics of Oscillations* ed J S Risley and R W Brehme (New York: American Institute of Physics)